

## Evaluation on bridge dynamic properties and VIV performance based on wind tunnel test and field measurement

Yongxin Yang<sup>1a</sup>, Tingting Ma<sup>\*2</sup> and Yaojun Ge<sup>1b</sup>

<sup>1</sup>State Key Lab for Disaster Reduction in Civil Engineering, Tongji University, Shanghai 200092, China

<sup>2</sup>College of Ocean Science and Engineering, Shanghai Maritime University, Shanghai 201306, China

(Received October 10, 2014, Revised February 11, 2015, Accepted February 20, 2015)

**Abstract.** Full scale measurement on the structural dynamic characteristics and Vortex-induced Vibrations (VIV) of a long-span suspension bridge with a central span of 1650 m were conducted. Different Finite Element (FE) modeling principles for the separated twin-box girder were compared and evaluated with the field vibration test results, and the double-spine model was determined to be the best simulation model, but certain modification still needs to be made which will affect the basic modeling parameters and the dynamic response prediction values of corresponding wind tunnel tests. Based on the FE modal analysis results, small-scaled and large-scaled sectional model tests were both carried out to investigate the VIV responses, and probable Reynolds Number effects or scale effect on VIV responses were presented. Based on the observed VIV modes in the field measurement, the VIV results obtained from sectional model tests were converted into those of the three-dimensional (3D) full-scale bridge and subsequently compared with field measurement results. It is indicated that the large-scaled sectional model test can probably provide a reasonable and effective prediction on VIV response.

**Keywords:** twin-box girder suspension bridge; dynamic characteristics; VIV response; FE modeling; sectional model test; field measurement; Reynolds Number effects

---

### 1. Introduction

Structural dynamic characteristics are fundamental parameters when conducting dynamic response analysis or wind-tunnel tests on wind-induced aero-elastic performance of long-span bridges. In the current procedure of wind-resistant design for long-span bridges, structural dynamic characteristics are calculated by Finite Element Methods and further used to determine fundamental parameters of spring-supported sectional model or full-bridge aero-elastic model wind tunnel tests. Consequently, any deviation of these calculated values from the dynamic characteristics of full-scale bridges may lead to errors in the predictions of structural aero-elastic behaviors.

Currently, single-spine, double-spine and triple-spine beam element models and shell element model have been developed to model bridge decks with different configurations in FE modal

---

\*Corresponding author, Ph.D., E-mail: [tingtinghorse@126.com](mailto:tingtinghorse@126.com)

<sup>a</sup> Associate Professor, E-mail: [yang\\_y\\_x@tongji.edu.cn](mailto:yang_y_x@tongji.edu.cn)

<sup>b</sup> Professor, E-mail: [yaojunge@tongji.edu.cn](mailto:yaojunge@tongji.edu.cn)

analysis, which were discussed in detailed (Zhu *et al.* 2000). Even there is an optimal deck model for bridges with different deck sections or different structural systems, inevitable deviation of dynamic characteristics exists between FE models and full-scale bridges (Ma and Ge 2014). For this purpose, field vibration tests, like ambient vibration test or forced vibration test, have been conducted to identify the actual modal properties and check the baseline FE models. Modal analysis and ambient vibration tests have been both carried out for several suspension bridges with super-long span, such as the Akashi Kaikyo Bridge in Japan (Katsuchi *et al.* 2004, 2006), the Great Belt Bridge in Denmark (Tanaka 1998, Brincker *et al.* 2000) and the Runyang Bridge in China (Wang *et al.* 2010). About 10% lower natural torsional frequencies compared with field measurement results were discovered in the modal analysis of the Akashi Kaikyo Bridge, which was attributed to the ignorance of the deck stiffness of the composite girder. For Runyang Bridge, the natural frequencies of lateral bending modes and torsional modes calculated with a single-spine beam element model are much lower than those measured from ambient vibration tests. Above mentioned comparative results all indicate that there are more or less differences in the natural frequencies of long-span bridges between FE modal analysis and full scale measurement. Moreover, frequently observed fluctuating modal damping ratios on site are quite different from the damping ratio which was set as a certain value in spring-supported wind tunnel tests. These all imply that some modifications should be adopted in the predictions of structural aero-elastic behaviors from the collaborative work of theoretical analysis and wind tunnel test.

As a kind of structural aero-elastic behaviors, Vortex-induced Vibrations (VIV) has attracted more and more attention in wind engineering to achieve better serviceability of bridges, particularly for bridges with twin-box girders. Laima *et al.* (2013) investigated the flow characteristics around a twin-box girder when undergoing vortex-induced vibration, based on which five schemes were designed to suppress the VIV of the twin-box girder. Long-term wind and wind effect monitoring system was also created to investigate the VIVs of a long-span suspension bridge with a twin-box girder (Li *et al.* 2011, 2014).

Wind tunnel test is considered to be a reliable way to predict VIV response provided that the experimental situation can adequately simulate full-scale conditions, including structural parameters (modal frequencies, damping ratios) and flow condition around the more or less bluff body, which, however, can hardly be realized perfectly. Li *et al.* (2014) investigated the VIVs of a long-span suspension bridge with a twin-box girder. The VIVs from a section model test and the full-scale bridge were compared, and it was found that the vertical VIV amplitude of the section model was much smaller than that from the field monitoring results. This study indicates that the wind direction, inflow turbulence and the inhomogeneity of the wind field along the span-wise direction of the bridge are critical factors that affect VIVs of the full-scale bridge. Some other researches focused on the conversion of the VIV amplitudes between the section model and the three-dimensional full structure (Zhang and Chen 2011, Sun *et al.* 2013)

In the present paper, field vibration tests on structural dynamic characteristics were carried out for a suspension bridge with a separated twin-box girder in China. Modal analysis results were compared with field testing results, and different modeling principles of FE model were compared and evaluated. Furthermore, small scaled and large scaled sectional model tests and full scale measurements on VIV responses were both conducted. The influence of structural parameters and Reynolds Number effects on VIV response prediction are finally discussed.

## 2. Twin-box girder suspension bridge

Connecting two large cities, Ningbo and Zhoushan, the Zhoushan Island-Mainland Connection Project has provided a major traffic line between China mainland and the archipelago city, and Xihoumen Bridge is the key part of this project, crossing the Xihoumen Channel, one of the most important deep waterways. A very long span is required in order to minimize bridge and environmental risks due to ship collision, technical complexity and unpredictable costs in constructing deep-water foundation. These requirements result in a suspension bridge with a 1650 m main span with steel box girder (Fig. 1), which has created a world record for box-girder suspension bridges. The bridge deck is composed of two separated steel box girders with 6 m central vent. The detailed geometry configuration of the deck section is shown in Fig. 2.

While the adoption of twin box girder can be an effective solution to improve the flutter stability of box-girder suspension bridges, more attention should be paid to the VIV performance of this girder section, since the existence of central vent will make vortex shedding process and its effect on structures more complicated. Besides, it is more challenging to acquire accurate FE modal analysis results due to the special layout of separated twin box girder.

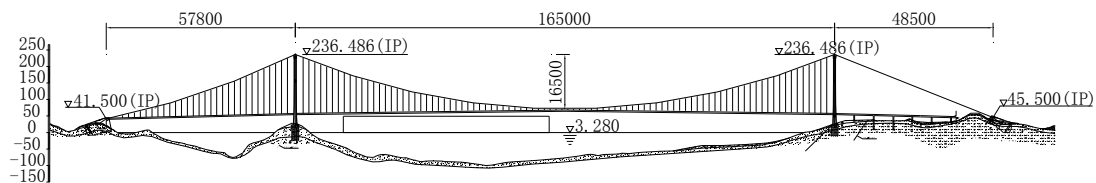


Fig. 1 Elevation of Xihoumen Bridge (Units for Size: cm; Units for Elevation: m)

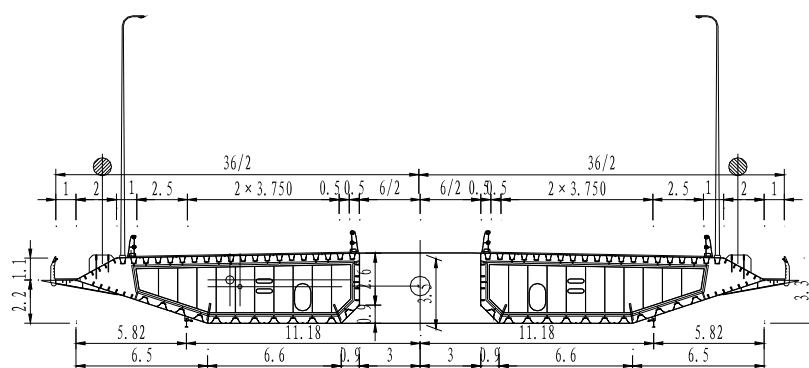


Fig. 2 Twin-box girder section of Xihoumen Bridge (Units: m)

### 3. Structural dynamic characteristics

#### 3.1 FE model

In the three-dimensional FE model of Xihoumen Bridge, pylons and piers are modelled by beam elements with six degrees of freedom (DOFs) at each node. The main cables and the suspenders are simulated by three-dimensional linear elastic truss elements with three DOFs at each node. Both the back cables and the towers are fixed at the base.

The modelling of bridge deck is more challenging for its typical separated twin-box section. The traditional single-spine model best suited for single box girder may present complexities in the calculation of equivalent stiffness. The deviation of the mass centroid of the whole girder section from the shear center of each single box will cause another simulation problem concerning axis positioning. Special attention was therefore paid to the establishment of a better FE deck model. Totally four kinds of deck models, including single-spine model (SG) with axis located at the mass centroid of the whole girder section, double-spine model with axes located at the mass centroid of each separated box (DG1), double-spine model with axes located at the shear center of each separated box (DG2) and four-spine model with axes both at the mass centroid and the shear center of each separated box (FG), are compared and evaluated. Fig. 3 illustrates the details of different FE deck models. The crossbeams are simulated by traditional 3D beam elements.

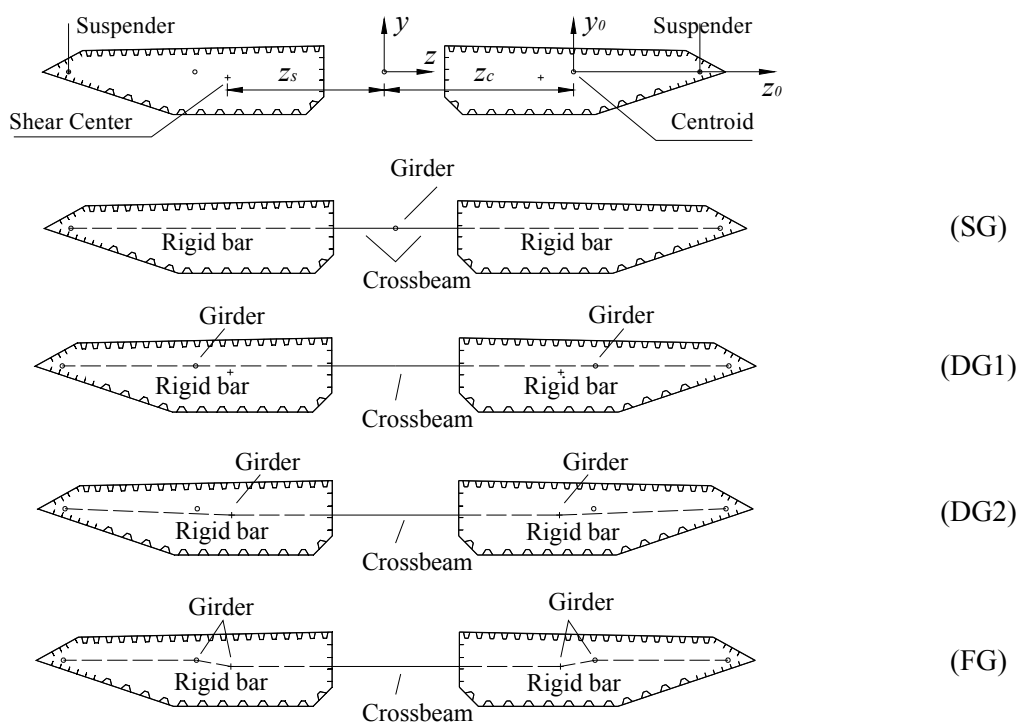


Fig. 3 Modeling details of different deck models

Table 1 Structural parameters of different deck models

Parameter	SG	DG1	DG2	FG
Axis Location	$(y=y_c, z=0)$	$(y=y_c, z=z_c)$ $(y=y_c, z=-z_c)$	$(y=y_s, z=z_s)$ $(y=y_s, z=-z_s)$	$(y=y_c, z=z_c, z=-z_c)$ $(y=y_s, z=z_s, z=-z_s)$
Tensile Rigidity	$2EA$	$EA$	$EA$	$EA(\text{Centroid})$
Vertical Bending Stiffness	$2EI_{z0}$	$EI_{z0}$	$EI_{z0}$	$EI_{z0} (\text{Centroid})$
Lateral Bending Stiffness	$2(EI_{y0}+EAz_c^2)$	$EI_{y0}$	$EI_{y0}$	$EI_{y0} (\text{Centroid})$
Torsional Stiffness	$2GJ_d$	$GJ_d$	$GJ_d$	$GJ_d(\text{Shear center})$
Distributed Mass	$2m$	$m$	$m$	$m(\text{Centroid})$
Distributed Mass Moment of Inertia	$2(I_m+mz_c^2)$	$I_m$	$I_m+m(z_c^2-z_s^2)$	$I_m (\text{Shear center})$

Note: subscripts *c* and *s* represent mass centroid and shear center, respectively.

Table2 Modal analysis results of Xihoumen Bridge (Units: Hz)

Mode Shape	SG	DG1	DG2	FG
1-S-L	0.0487	0.0485	0.0469	0.0485
1-AS-L	0.1106	0.1094	0.0998	0.1094
1-AS-V	0.0787	0.0791	0.0791	0.0791
1-S-V	0.1005	0.1005	0.1005	0.1005
1-S-T	0.2145	0.2321	0.2284	0.2321
1-AS-T	0.2132	0.2371	0.2312	0.2371

Note: S-symmetric, AS-asymmetric, L-lateral bending, V-vertical bending, T-torsion

The principal parameters of different deck models are listed in Table 1. Parameters  $A, I_{z0}, I_{y0}, J_d$  represent the area, the vertical bending moment of inertia, the lateral bending moment of inertia, the free torsional moment of inertia of each separated single box girder, respectively.  $m$  and  $I_m$  denote the mass and the mass moment of inertia per unit length (along the bridge longitudinal axis) around its mass centroidal axis for each separated box section, respectively.

Based on the FE models developed above, modal analysis was performed and principal results of natural frequencies are shown in Table 2. These results indicate that DG1 is equivalent to FG. For twin-box section with boxes connected by crossbeams, the real lateral bending stiffness ranges between  $2EI_{y0}$  and  $2(EI_{y0}+EAz_c^2)$ . It can be observed in Table 1 that SG overestimates the lateral

bending stiffness, which results in overestimated lateral vibration frequencies. But for DG2, underestimated lateral bending frequencies are obtained compared with DG1. As shown in Fig. 3, compared with the mass centroid of each single box, the shear center is closer to the mass centroidal axis of the whole girder section ( $z_s < z_c$ ), which results in a smaller lateral bending stiffness and hence a lower frequency of each lateral bending mode. It can be concluded that SG and DG2 are inappropriate in lateral stiffness modelling for twin box girders. On the other hand, vertical bending frequencies show little differences between different deck models. The difference in torsional frequencies between these deck models can be attributed to the different simulation of section warping effects since the mass moment of inertia of the whole twin-box girder section for different deck models are the same, as shown in Table 1. The warping effects have not been considered in SG, while for either DG1 or DG2, the warping stiffness is represented by the vertical bending stiffness of each single box times the square of the horizontal distance between the axis of each spine and the center of the whole girder section, which lead to higher torsional frequencies. Compared with DG2, the contribution of section warping effect is higher for DG1 model due to the fact that  $z_s < z_c$ . In summary, DG1 model can be recommended to model separated twin-box girder for its reasonability and simplicity in FE modelling.

### 3.2 Field vibration test

The modal testing and measurement of a bridge on site provide accurate and reliable predictions of its global modal parameters, including natural vibration modes, natural frequencies and modal damping ratios. In order to verify the FE modal analysis results and to identify the structural damping, field vibration tests consisting of both forced vibration test and ambient vibration measurement were carried out for the Xihoumen Bridge.

#### 3.2.1 Forced vibration test

The forced vibration test was conducted particularly for several vertical bending modes since heaving VIV was observed on site right after guard rails were erected on the deck. The test was therefore carried out during the finished bridge state. The wind speed during the test was below 1m/s. The excitation of the forced vibration test was generated by a group of 200 workers, who located at mid-span, 1/4 span, 1/8 span and jumped at a specific frequency with the help of metronomes.

The modal damping ratios were identified with Logarithmic Decrement (LD) method. After the artificial excitation, the response of the bridge presented a damped free vibration. The modal damping ratio  $\xi$  can be expressed as

$$\xi \approx \frac{1}{2m\pi} \ln \frac{v_n}{v_{n+m}} \quad (1)$$

where  $v_n$  and  $v_{n+m}$  represent the  $n^{\text{th}}$  and  $(n+m)^{\text{th}}$  peak values of the vibration curve, respectively.

#### 3.2.2 Ambient vibration test

The ambient vibration test of the Xihoumen Bridge was also performed after the completion of bridge deck pavement and guard rail installation (Ge and Yang 2011). The wind speed during the test ranged from 2 m/s to 8 m/s, while the temperature varied between 25 °C and 30 °C. A wireless vibration testing and data acquisition system was employed for vibration identification of the deck

and the main cables. A rather dense measurement layout on the deck in the vertical and lateral direction was employed to identify better vibration mode shapes of the bridge. As a result, there are totally 50 vertical and 25 lateral accelerometers set on the bridge deck. Besides, 14 vertical and 7 lateral accelerometers are located along the main cables, and 18 measuring points on the bridge pylon. The detailed layout of the measurement points on the deck, the main cables and the towers are shown in Fig. 4.

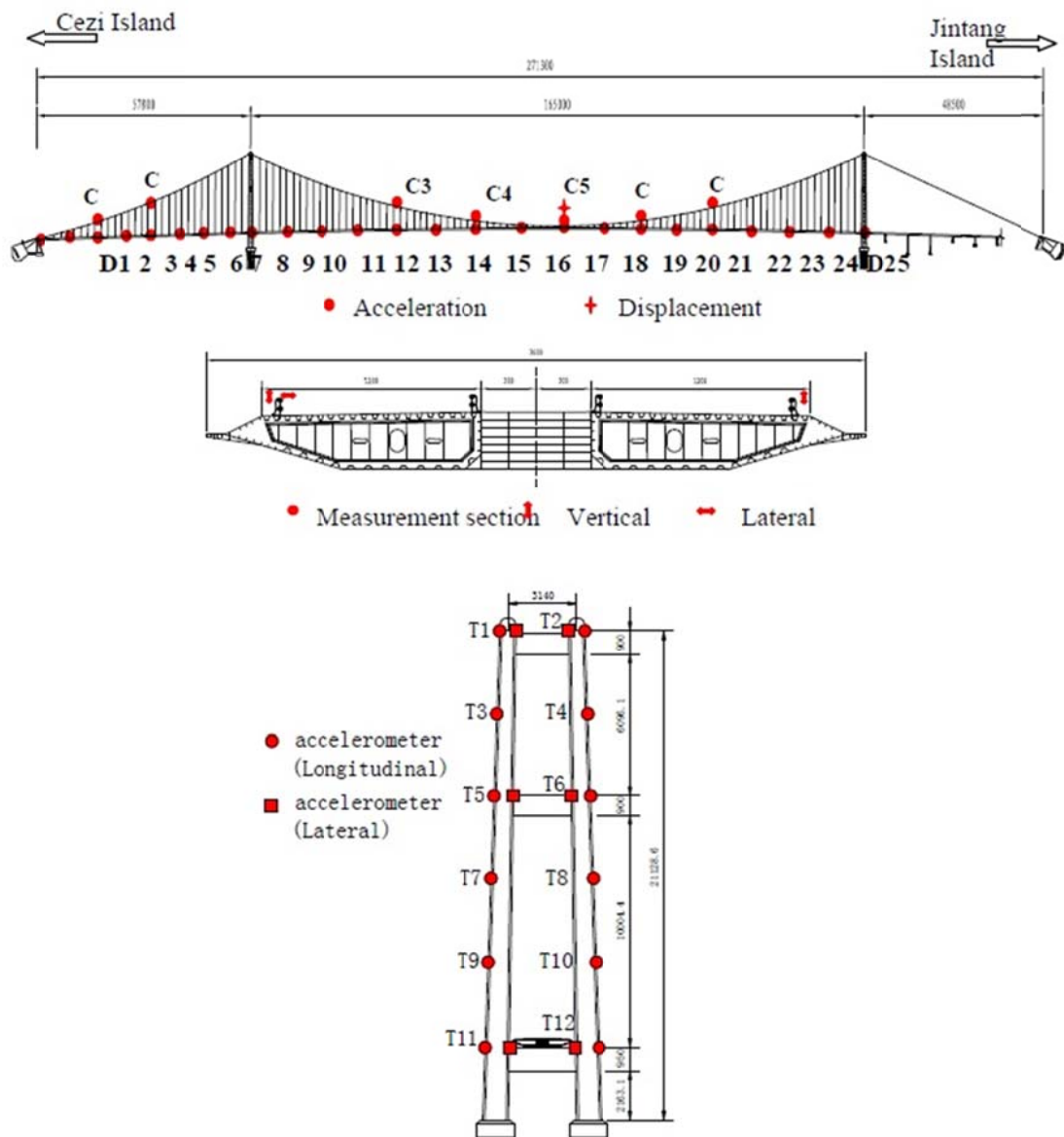


Fig. 4 Layout of measurement points

Table 3 Comparison of modal parameters of Xihoumen Bridge

No.	Ambient vibration tests			Forced vibration tests		Calculated	Mode shape
	Frequency (Hz)	Damping ratio (%)		Frequency (Hz)	Damping ratio (%)	Frequency (Hz)	
		EFDD Method	SSI Method		LD Method		
1	0.054	1.42~2.60	1.95~2.25	-	-	0.0485	1-S-L
2	0.095	1.12~2.64	1.80~2.18	-	-	0.0791	1-AS-V
3	0.103	1.39~2.33	1.02~1.62	-	-	0.1005	1-S-V
4	0.123	0.82~2.54	1.54~2.02	-	-	0.1094	1-AS-L
5	0.133	0.84~2.32	0.90~1.46	0.135	0.47~0.85	0.1328	2-S-V
6	0.183	0.18~1.02	0.37~0.61	0.180	0.49~0.92	0.1787	2-AS-V
7	0.202	0.38~0.64	0.28~0.48	-	-	0.1868	Cable
8	0.208	0.23~0.57	0.43~0.67	-	-	0.1872	2-S-L
9	0.209	0.22~0.68	0.18~0.60	-	-	0.1955	Cable
10	0.229	0.27~0.65	0.48~0.94	0.230	0.41~1.17	0.2293	3-S-V
11	0.229	0.21~0.59	0.23~0.62	-	-	0.2321	1-S-T
12	0.233	0.25~0.41	0.77~0.95	-	-	0.2371	1-AS-T
13	0.268	0.16~0.94	0.21~0.43	-	-	0.2610	1-AS-V (Side span)
14	0.276	0.34~1.14	0.43~0.83	0.275	0.39~0.46	0.2739	3-AS-V
15	0.327	0.35~0.63	0.36~0.68	-	-	0.3245	4-S-V
16	0.349	0.40~0.82	0.42~0.88	-	-	0.3487	2-S-T
17	0.379	0.09~0.75	0.44~0.72	-	-	0.3751	4-AS-V
18	0.380	0.16~0.60	0.17~0.51	-	-	0.3755	2-AS-L
19	0.418	0.15~0.65	0.28~0.84	-	-	0.4031	1-S-V (Side span)
20	0.435	0.25~0.79	0.21~0.37	-	-	0.4295	5-S-V

Note: S-symmetric, AS-asymmetric, L-lateral bending, V-vertical bending, T-torsion

The Enhanced Frequency Domain Decomposition (EFDD) technique and the Stochastic Subspace Identification (SSI) method in time domain were used to identify modal parameters. The EFDD method is an extension of the original Frequency Domain Decomposition (FDD) method. The basis of this method is creating the spectral density matrix of the response and then performing singular value decomposition. Under some assumptions (white noise excitation, low damping and orthogonal mode shapes for close modes), the singular values of the spectral matrix are auto-spectral density functions of single degree of freedom systems. From auto-correlation functions, which can be calculated by applying an inverse fast Fourier transform to the auto-spectral density functions, it is straightforward to identify the modal damping ratios and obtain enhanced estimates of the natural frequencies. These frequencies are evaluated looking at the time intervals between zero crossings. The modal damping ratios are estimated adjusting an exponential decay to the relative maxima of the auto-correlation functions. Mode shapes are identified from the singular vectors of the spectral matrix evaluated at the identified resonance frequencies and associated with the singular values that contain the peaks (Magalhães *et al.* 2010). SSI is an output-only time domain method that directly works with time data, without the need to convert them to correlations or spectra. The method is especially suitable for operational modal

parameter identification. A more detailed description of SSI method can be found in the work developed by Döhler *et al.* (2014).

### 3.2.3 Measured results and comparison

The frequencies, damping ratios of totally four vertical bending modes were identified in the forced vibration tests, while in the ambient vibration tests, totally 32 natural vibration modes were identified. The measured frequencies and damping ratios are listed and compared with the FE analysis results (double-spine model DG1), as shown in Table 3.

Generally, the calculated modal frequencies agree well with the measured results except for the lateral bending modes and the first asymmetric vertical mode. The obviously lower calculated frequencies of the lateral bending modes can be probably attributed to the released longitudinal constraints at the sliding bearings, which connect the deck to the tower cross-beam and the abutment. These bearings allow movements along the longitudinal direction of the bridge and rotation around the vertical axis. However, for low-level (ambient) dynamic response, the behavior of these connections can be different (Magalhães *et al.* 2008). It is always assumed that relative translational motions between deck and tower would not occur and that the only relative motion possible was a free rotation of the deck with respect to tower cross-beam (longitudinal bending) (Wilson and Gravelle 1991). Furthermore, the longitudinal dampers may possibly contribute to the constraint for the longitudinal movements of the girder.

Therefore, modal analysis was conducted by the modified FE model with longitudinal constraints at each of those bearings. The frequency of the first asymmetric vertical bending mode increased to 0.0939 Hz, while the frequencies of the first symmetric and asymmetric lateral bending modes changed to 0.0562 Hz and 0.1287 Hz, respectively. The refined FE model presents better agreement with the field measurement results.

## 4. Vortex-induced vibrations

### 4.1 Small scaled sectional model testing

Traditional small scaled girder sectional model wind tunnel test was firstly conducted to evaluate the VIV performance of the twin box girder for the Xihoumen Bridge, as shown in Fig. 5. The wind tunnel test was carried out in the TJ-1 Boundary Layer Wind Tunnel (overall size of 12 m length, 1.8 m width and 1.8 m height) in Tongji University, under the smooth flow condition. This small scaled sectional model is 1.7 m long and 0.9 m wide, adopting a geometrical scale of 1:40. The wind velocity scale of 1:1.5 was selected. The sectional model was supported by 8 springs. The frequencies of the first symmetric heaving and torsional modes resulted from FE modal analysis (Table 3) were scaled and applied to the sectional model. The equivalent mass and mass moment of inertia of the sectional model are 17.194 kg/m and 1.564 kg·m<sup>2</sup>/m, respectively. The damping ratio of the sectional model is 0.45% for the heaving mode and 0.3% for the torsional mode.

No heaving VIV response was detected, while torsional VIV responses were observed at 0° and +3° wind angle of attack with almost the same lock-in range of [7.5 9.9]m/s, which are shown in Fig. 6. The VIV responses as well as the wind velocity in Fig. 6 have been transferred to the full scale condition. The Strouhal number  $St$  ( $St = f_v D/U$ ,  $f_v = 6.190\text{Hz}$  is the vortex shedding frequency,  $D=0.0875$  m is the center height of the twin-box girder, and  $U = 7.5/1.5 = 5$  m/s is the

inflow velocity) of the 1:40 sectional model test is 0.1083 for both  $0^\circ$  and  $+3^\circ$  wind angle of attack. Note that the  $f_v$  and  $U$  used here corresponds to the starting point of the lock-in region. According to the lock-in theory,  $f_v$  is equal to the mechanical frequency of the suspension system. The Reynolds number  $Re$  ( $Re = UD/\nu$ , where  $U$  is the inflow velocity,  $D$  is the center height of bridge deck, and  $\nu = 0.0000148$  is the kinematic viscosity) at the torsional VIV condition ( $U = 5$  m/s~6.6 m/s) is in the range of [29561 39020].

#### 4.2 Large scaled sectional model testing

For further detailed investigation on VIV responses, a combination of geometry, mass, stiffness and Reynolds number considerations resulted in the selection of a 1:20 geometrical scale for the sectional model, which has a total length of 3.6 m and a width of 1.8 m (Yang and Ge 2012). The wind velocity scale of 1:1 was selected. The dynamic properties of this sectional model, with a vertical frequency of 2.010 Hz and a torsional frequency of 4.642 Hz, are scaled from the FE modal analysis results corresponding to the first symmetric heaving and torsional modes. The equivalent mass and mass moment of inertia are 68.778 kg/m and 25.018kg·m<sup>2</sup>/m, respectively. The wind tunnel testing was conducted in smooth flow at Tongji University's TJ-3 Boundary Layer Wind Tunnel with the working section of the 15 m width, the 2 m height and the 14 m length. Two rigid and streamlined temporary end walls were designed and built in the working section to accommodate the large sectional model (Fig. 7), and the suspension system including 8 springs and supporting frames was built in these two end walls together with 4 optical laser displacement transducers for the measurement of the response of the sectional model to vortex-shedding excitation. Different damping conditions were considered in the tests. The variation of the damping was achieved by mechanical dampers, which are composed of a plastic bar with one end tied to the arms of the suspension system and the other connected with a small mass. Different damping cases were realized by adjusting the length of the plastic bar.



Fig. 5 Small scaled sectional model test

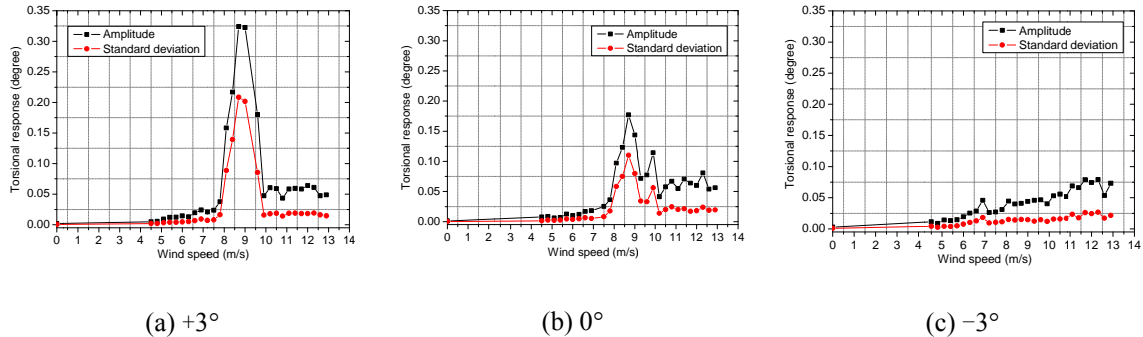


Fig. 6 VIV responses in small scaled sectional model testing



Fig. 7 The 1:20 girder sectional model

Different from the results obtained from small scaled sectional model testing, the VIV responses in both heaving and torsional DOF were observed in the testing. The Strouhal number corresponding to the torsional VIV are 0.1083, 0.1083 and 0.1015 for +3°, 0° and -3° wind angle of attack, respectively, while for the vertical VIV, are 0.2345, 0.2069 and 0.1954, respectively. The Reynolds number based on the center height of bridge deck at the heaving VIV condition ( $U = 1.5 \text{ m/s} \sim 3.7 \text{ m/s}$ ) is in the range of [17736 43750]. The Reynolds number at the torsional VIV condition ( $U = 7.5 \text{ m/s} \sim 12.0 \text{ m/s}$ ) is in the range of [88682 141892]. The comparisons between girders with different structural damping ratios at +3°, 0°, -3° wind angle of attack are illustrated in Fig. 8, which indicate that the structural damping has great influence on the amplitude of VIV response.

By comparing with large scaled sectional model test results, the phenomenon that only torsional VIV response was observed in small scaled sectional model test may be attributed to two primary reasons. One reason may be attributed to the lowest stable inflow velocity (about 2 m/s) of TJ-1 Boundary Layer Wind Tunnel. It can be seen from Fig. 8 that the lock-in range for heaving VIV is about [1.5 m/s 3.7 m/s], according to which, the lock-in range of [1 m/s 2.47 m/s] of the small scaled sectional model test is expected. However, the lowest stable inflow velocity of 2m/s generally cannot meet the occurrence conditions of VIVs. The other reason may be attributed to

the Reynolds number effect and scale effect. In the research carried out by Li *et al.* (2014), the rough flow pattern around the lower surface of the twin-box girder was presented based on the flow visualization of a 1:25 sectional model (a geometry scale close to 1:20). This research indicates that the flow separates at the lower surface of the rail accompanied with large vortex shedding, and then the leading vortex propagates downstream and merges with vortices that are created at the trailing edge of the downstream box girder, finally forming the Karman-like vortices in the wake. However, the Reynolds number of the expected vertical VIV region for the 1:40 sectional model, in the range of [5912 14583], is only one third of that of the 1:20 sectional model. The flow separation and reattachment may probably be much different under such low Reynolds number conditions. The detailed mechanisms will be further studied in the future by the authors.

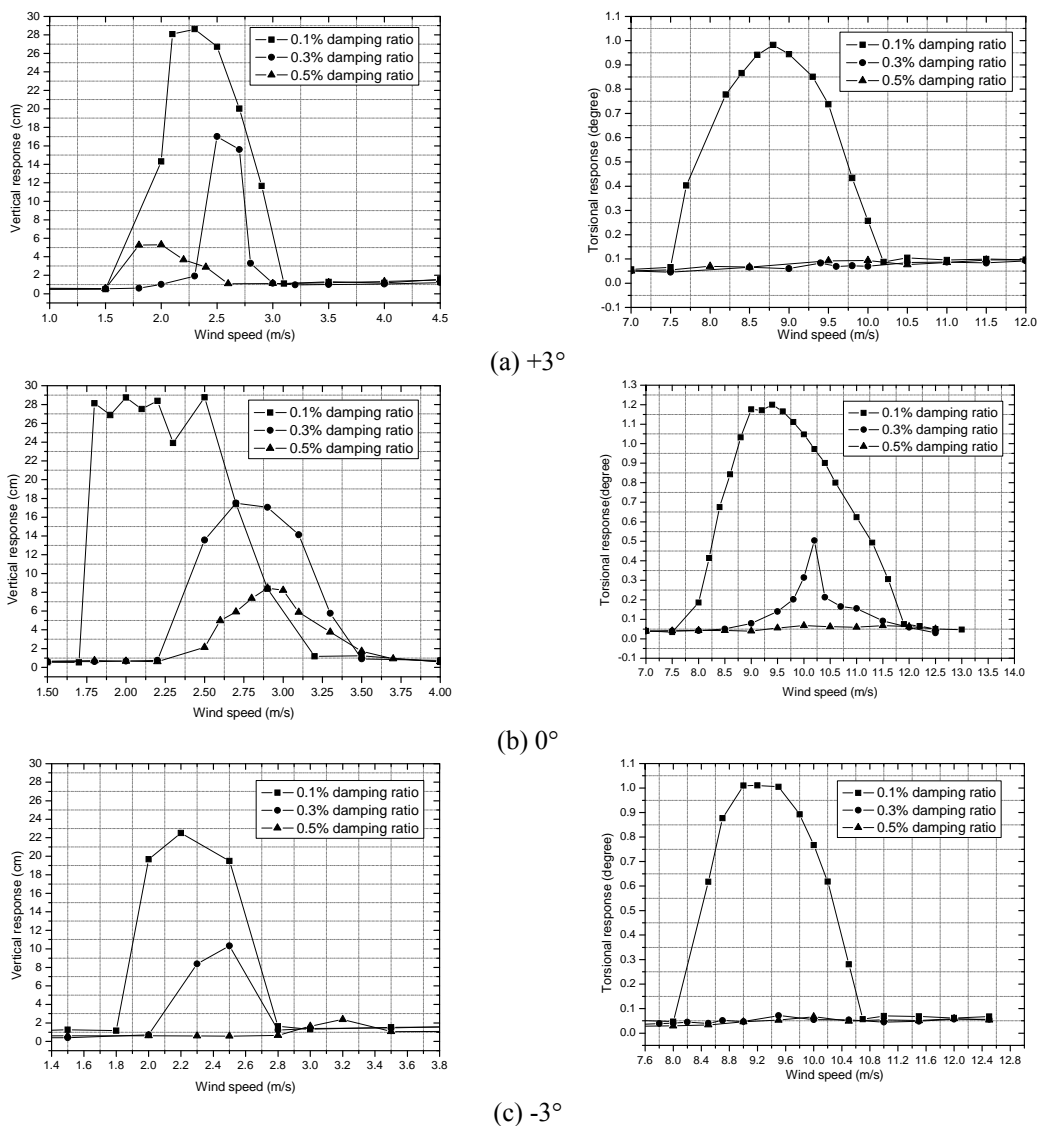


Fig. 8 VIV responses of girders with different damping ratios

### 4.3 Field measurement on VIV responses

Heaving VIV response of twin box girder was observed on site after guard rails were erected on the deck for the first time (Ge and Yang 2011). The vibration process was recorded, and Fig. 9 presents typical screenshots taken from the recorded video.

From the recorded VIV video, the VIV frequency and the oscillation amplitude of the deck near the north pylon can be detected as 0.32 Hz and 5.0 cm respectively. The VIV mode is probably the 4th symmetric heaving mode according to Table 3, with corresponding damping ratio ranging between 0.35% and 0.63%. Based on the vibration mode shapes, the maximum VIV amplitude of 16.3 cm can be estimated as illustrated in Fig. 10.

After that, four accelerometers were installed on the girder deck, among which two at mid span, and one at 3/8 and 1/4 span, respectively. The layout of these accelerometers is shown in Fig. 11.

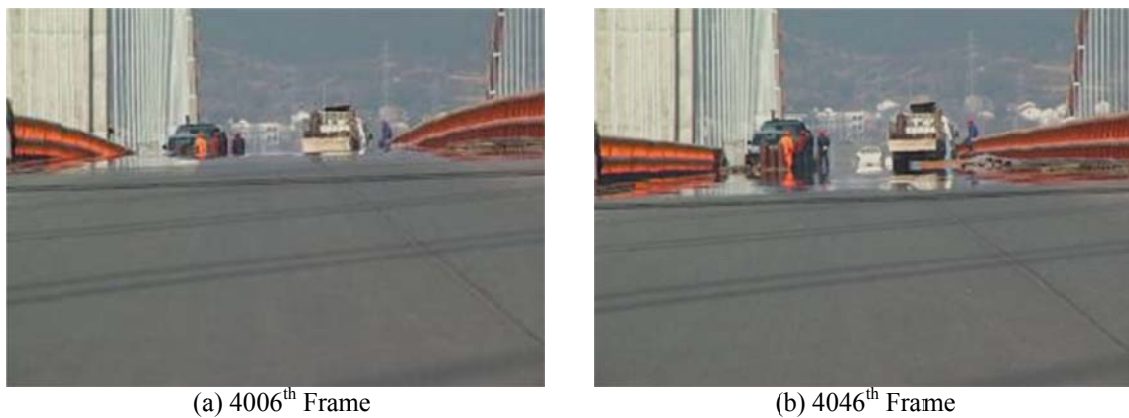


Fig. 9 Screenshots from videos recording VIV response (near the north pylon)

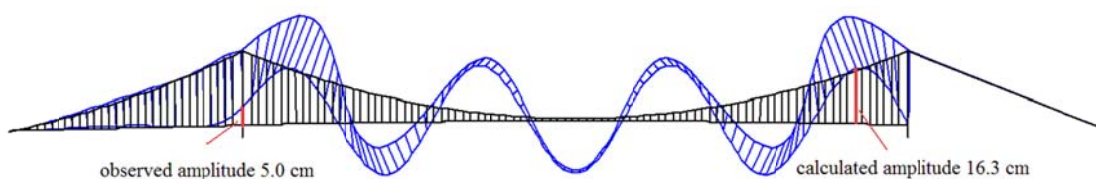


Fig. 10 VIV mode and maximum amplitude estimation

Table 4 Statistic results of measured vertical accelerations on the deck ( $\text{cm/s}^2$ )

Case Measuring Point	No VIV			During VIV		
	Max	Min	RMS	Max	Min	RMS
1 (mid span)	4.6	-4.7	2.5	38.3	-38.4	21.8
2 (mid span)	3.9	-4.2	1.7	36.4	-36.8	21.6
3 (1/8 span)	2.1	-2.2	0.6	9.3	-9.6	5.2
4 (1/4 span)	3.1	-3.6	0.9	12.6	13.2	7.1

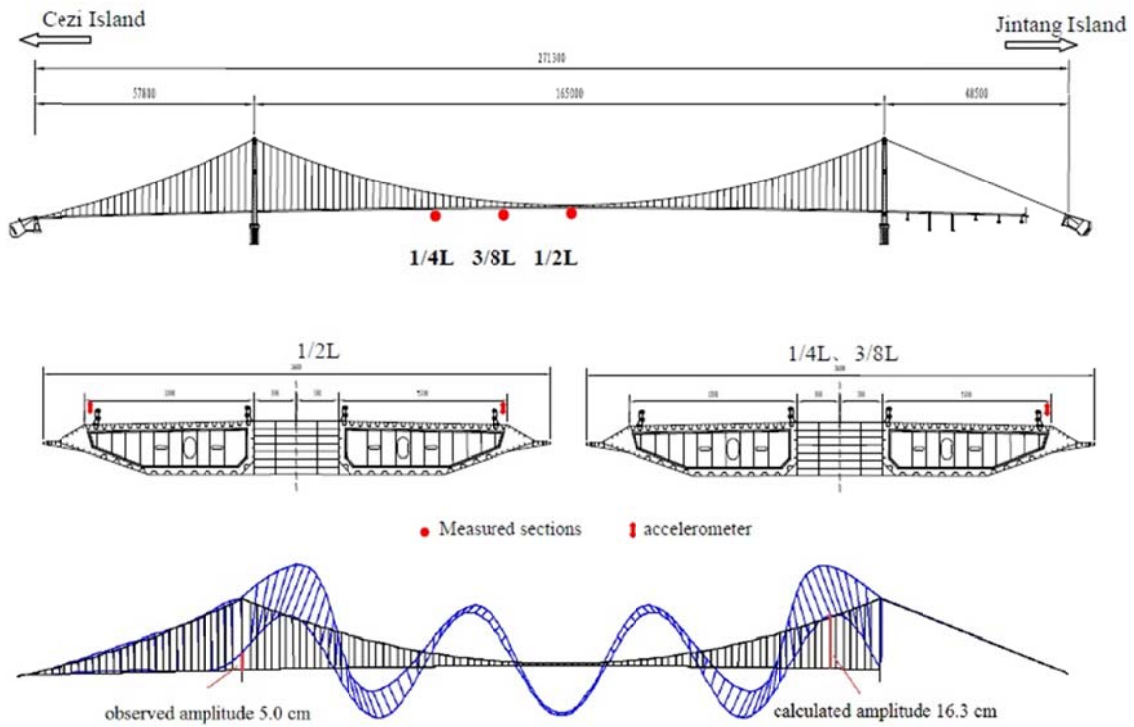


Fig. 11 Layout of accelerometers installed on the deck for VIV observation

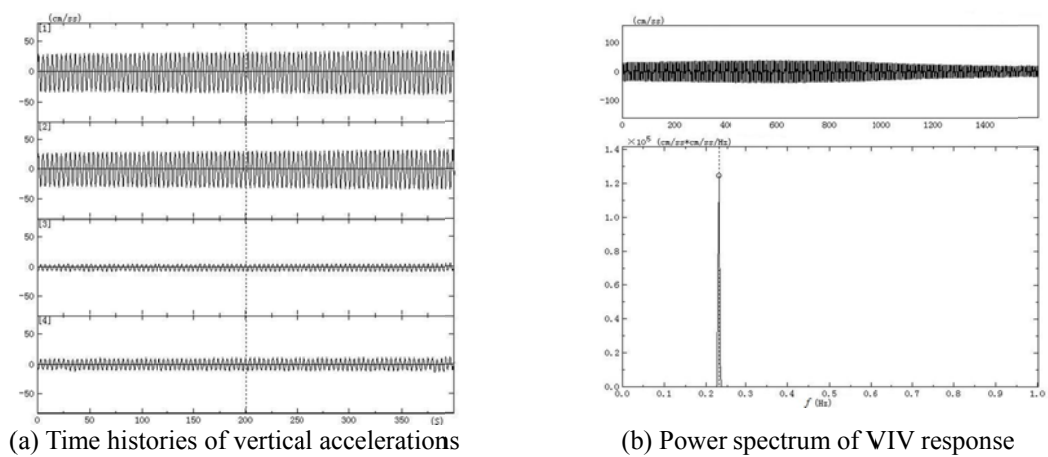


Fig. 12 Results of VIV field measurement

Table 5 Statistic results of vertical displacements on the deck (cm)

Measuring Point	Case	During VIV	
		Max	Min
	1 (mid span)	18.3	-18.4
	2 (mid span)	17.4	-17.6
	3 (3/8 span)	4.5	-4.6
	4 (1/4 span)	6.0	6.3

Table 6 Scale ratio to the 1st symmetric heaving mode

Mode shape	$\lambda_f$	$\lambda_V$
3-S-V	2.2977	2.2977
4-S-V	3.1968	3.1968

Three days later, heaving VIV response lasting about 90 minutes was captured. The wind speed during that day ranged from 2 m/s to 9 m/s. The time histories of vertical accelerations at four measuring points on the deck during VIV process and the power spectrum of VIV response at mid span of the deck are shown in Fig. 12. The statistic results of measured vertical accelerations and vertical displacements at these four measuring points are listed in Table 4 and Table 5 respectively. According to these results, the VIV frequency is 0.23 Hz and the amplitude reaches 18.4 cm.

According to the field measurement results of the structural modal properties shown in Table 3, the observed VIV mode corresponds to the 3rd symmetric heaving mode with modal damping ratio located between 0.27% and 0.65% (EFDD method).

#### 4.4 Discussions

As discussed earlier, the Reynolds number effect and the objective condition of the wind tunnel may probably influence the prediction of VIV response, which suggests that the largest possible geometrical and wind velocity scale in sectional model tests should be adopted for better VIV prediction.

To evaluate the effectiveness of large scaled sectional model test on VIV prediction, the test results were compared with the field measurement results. Firstly, the VIV response with respect to the first symmetric heaving mode in the wind tunnel test, as shown in Fig. 8, needs to be transformed into those for the 3rd and 4th symmetric heaving modes, which were observed on site as the VIV modes. The equivalent modal mass of the 1st, 3rd and 4th symmetric heaving modes are 27511 kg/m, 26320 kg/m and 25922 kg/m, respectively, which shows negligible differences between each other. Therefore, the influence of the differences in Scruton number ( $Sc$ ) on VIV amplitude was not taken into account. The three damping ratio cases (0.1%, 0.3% and 0.5%) in Fig. 8 are converted to the full scale condition with the amplitudes unchanged based on the Scruton theory. The frequency scale  $\lambda_f$  and velocity scale  $\lambda_V$  of these two modes relative to the 1st symmetric heaving mode are listed in Table 6. Based on these relative wind speed scale ratio, the lock-in wind speed range (Fig. 8) of the VIV responses predicted for the 1st symmetric heaving

mode has been shifted and enlarged as predicted VIV responses for the 3rd and 4th symmetric heaving mode.

The second step is to convert VIV responses from 2D bridge girder section to 3D full structure. The conversion formula proposed by Zhang (Zhang *et al.* 2014) based on the linear model of vortex-induced loading was adopted

$$\lambda_i = \frac{y_{3D_i}}{y_{2D}} = \varphi(x_i) \frac{\int_0^L |\varphi(x)| dx}{\int_0^L \varphi^2(x) dx} \quad (2)$$

where  $\lambda$  is the conversion coefficient;  $y$  represents VIV response;  $i$  denotes node number;  $\varphi(x)$  is the mode shape function. Based on the results in Table 6 and Eq. (2), the VIV response obtained from the large scaled sectional model test was converted into the responses of the 3D full bridge girder with respect to the 3rd and 4th symmetric heaving modes. According to FE modal analysis results, the conversion coefficients of the 3rd symmetric heaving mode are 1.4756, 0.3793 and 0.6748 for nodes located at mid-span, 3/8 span and 1/4 span, respectively, while for the 4th symmetric heaving mode, the conversion coefficient of the node with the maximum amplitude as shown in Fig. 10 is 1.3211.

The converted vibration amplitudes and wind speed ranges of VIV for the 3rd and 4th symmetric heaving modes are illustrated in Figs. 13 and 14, respectively, and compared with corresponding field measurement results. Since the exact wind velocity and wind angle of attack during VIV have not been exactly measured for some difficulties, the measured VIV responses on-site are depicted as red dotted lines covering the whole wind velocity range concerned.

Although the exact wind velocity and wind angle of attack during VIV were unknown, the VIV lock-in region as shown in Fig. 13 is about [3.5 9] m/s, which is close to the wind velocity range of [2 9] m/s measured on-site. This indicates that the large scaled sectional model test realized the prediction of the occurrence of VIVs and provided a reasonable lock-in region. Additionally, it can be found in Fig. 13 that the VIV amplitude obtained from field measurement generally locates between the curves corresponds to the 0.3% and 0.5% damping ratio. The field measured damping ratio of the 3rd symmetric heaving mode ranges between 0.27% and 0.65%, which overlaps with range of [0.3% 0.5%] to some extent. Similar results are presented in Fig. 14 for the 4th symmetric heaving mode. This indicates the reasonable prediction of the large scaled sectional model test on VIV amplitude. In other words, the reasonable and effective prediction of VIV will probably be obtained by the large scaled sectional model test, provided that the basic modeling parameters based on modal analysis are correct, and the conversion from wind tunnel tests to 3D full bridge concerning VIV amplitude and lock-in wind velocity range has been performed appropriately.

However, there remain many difficulties in carrying out more persuasive comparison between wind tunnel test and field measurement, such as the uncertain structural damping, the influence of turbulence, the measurement accuracy of the wind velocity on-site, the limitation in the conversion theory from 2D to 3D, and so on. All these factors need detailed and deep study in the future.

## 5. Conclusions

FE modelling principles of the twin box girder in the Xihoumen Bridge was compared and evaluated by comparison with the on-site identification results. It can be concluded that the

separated twin box girder can be best modelled by double-spine deck model with two beam element located at the centroid of each single box, but certain refinement of the FE model still needs to be performed based on field modal identification results, which will affect the basic modelling parameters and hence the dynamic response prediction values of corresponding wind tunnel tests. VIV performance of the twin box girder was investigated through traditional sectional model and large scaled model wind tunnel tests. The Reynolds Number effect or scale effect may probably affect the occurrence of VIV and corresponding amplitude. Comparative study with field measurement results indicates that the traditional sectional model test may lead to an unsafe prediction in VIV response, while for the large scaled sectional model test, the reasonable and effective prediction of VIV response can be obtained if the basic modelling parameters based on modal analysis are correct, and the conversion from wind tunnel tests to 3D full bridge can be appropriately realized.

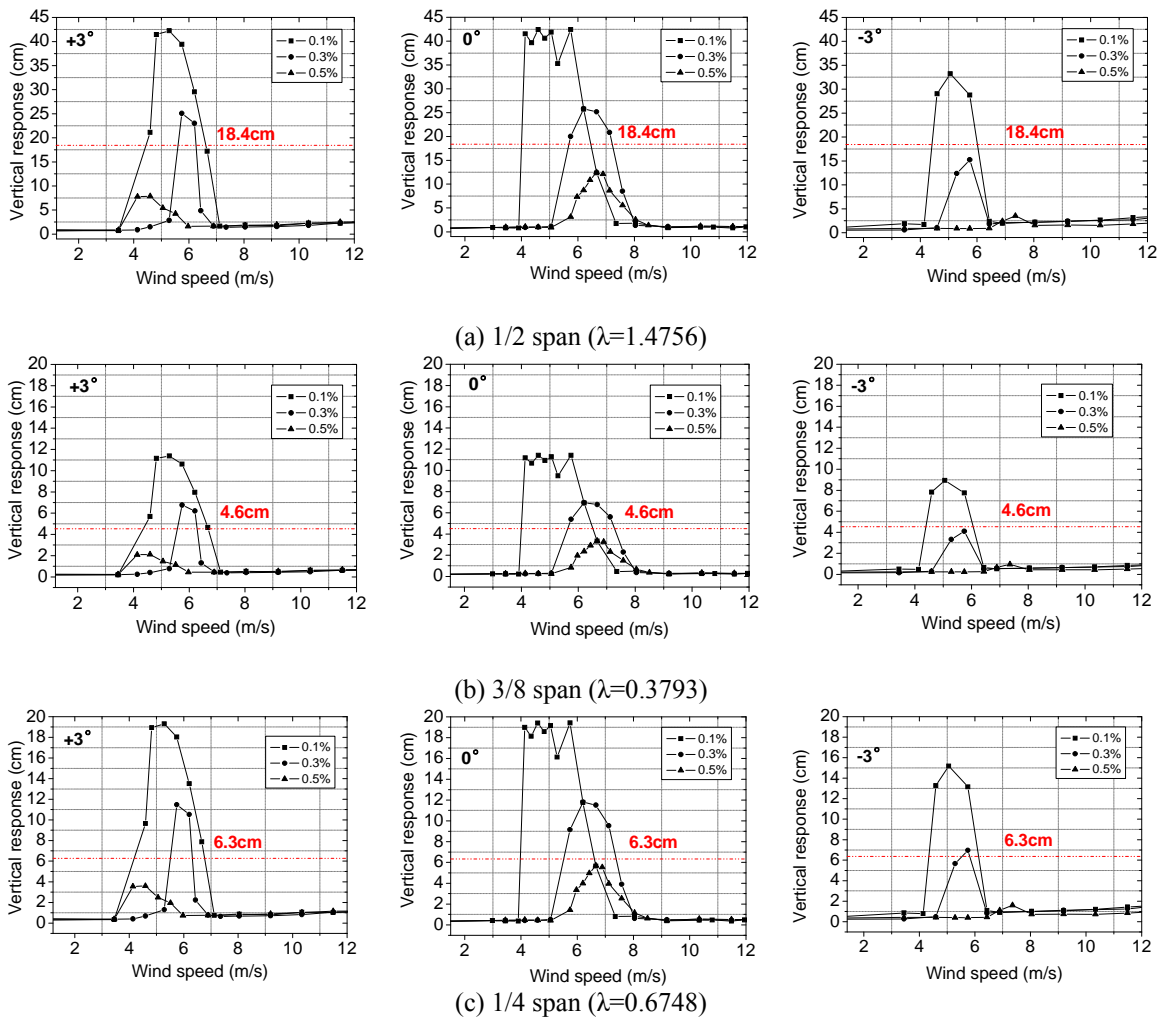


Fig. 13 VIV amplitude with different damping ratios (3-S-V)

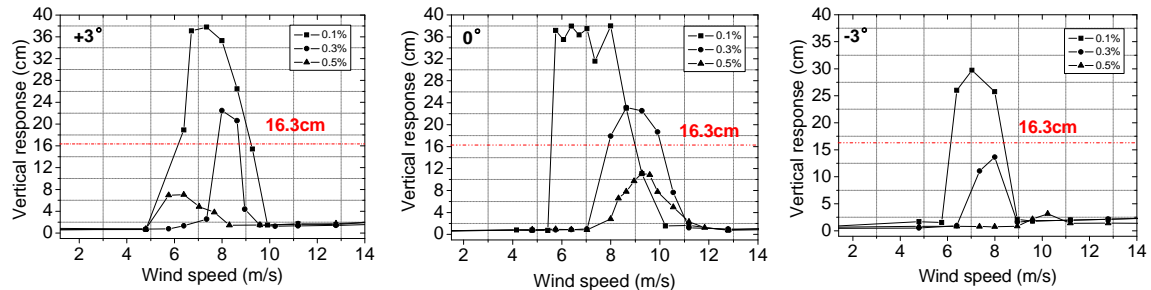


Fig. 14 Maximum VIV amplitude with different damping ratios (4-S-V) ( $\lambda=1.3211$ )

## Acknowledgements

The support for the research work jointly provided by the NSF Grant # 51078276 and research funding Grant # KLWRBMT-04 and SLDRCE 10-B-05, is gratefully acknowledged.

## References

- Brincker, R., Frandsen, J.B. and Andersen, P. (2000), "Ambient response analysis of the Great Belt Bridge", *Proceedings of the International Modal Analysis Conference - IMAC*, San Antonio, February.
- Döhler, M., Hille, F. Mevel, L. and Rücker, W. (2014), "Structural health monitoring with statistical methods during progressive damage test of S101 Bridge", *Eng. Struct.*, **69**, 183-193.
- Ge, Y.J., Yang, Y.X. and Cao, F.C. (2011), "Vortex shedding and its induced vibration of Xihoumen Suspension Bridge with twin box girder based on wind tunnel model testing and field measurement", *Proceeding of the 13th International Conference on Wind Engineering*, Amsterdam, July.
- Katsuchi, H., Yamada, H., Hata, K. and Kusuhara, S. (2004), "Full-scale Monitoring of Akashi-Kaikyo Bridge", *Proceedings of the 3rd China-Japan-US Symposium on Health Monitoring and Control of Structures*, Dalian, October.
- Katsuchi, H., Yamada, H. and Kusuhara, S. (2006), "Modal-damping Identification of Akashi Kaikyo Bridge by Wavelet Screening", *Proceedings of 4th China-Japan-US Symposium on Structural Control and Monitoring*, Hangzhou, October.
- Laima, S.J., Li, H., Chen, W.L. and Li, F.C. (2013), "Investigation and control of vortex-induced vibration of twin box girders", *J. Fluids Struct.*, **39**, 205-221.
- Li, H., Laima, S.J., Ou, J.P., Zhao, X.F., Zhou, W.S., Yu, Y., Li, N. and Liu, Z.Q. (2011), "Investigation of vortex-induced vibration of a suspension bridge with two separated steel box girders based on field measurements", *Eng. Struct.*, **33**(6), 1894-1907.
- Li, H., Laima, S.J., Zhang, Q.Q., Li, N. and Liu, Z.Q. (2014), "Field monitoring and validation of vortex-induced vibrations of a long-span suspension bridge", *J. Wind Eng. Ind. Aerod.*, **124**, 54-67.
- Ma, T.T. and Ge, Y.J. (2014), "Uncertainty effects of structural FE model and turbulent wind loading on bridge buffeting response", *J. Struct. Eng. (India)*, **41**(1), 1-10.
- Magalhães, F., Cunha, Á. and Caetano, E. (2008), "Dynamic monitoring of a long span arch bridge", *Eng. Struct.*, **30**(11), 3034-3044.

- Magalhães, F., Cunha, Á., Caetano, E. and Brincker, R. (2010), "Damping estimation using free decays and ambient vibration tests", *Mech. Syst. Signal Pr.*, **24**(5), 1274-1290.
- Sun, Y.G., Li, M.S. and Liao, H.L. (2013), "Investigation on vortex-induced vibration of a suspension bridge using section and full aeroelastic wind tunnel tests", *Wind Struct.*, **17**(6), 565-587.
- Tanaka, H. (1998), *Wind Engineering*. University of Ottawa.
- Wang, H., Li, A.Q. and Li, J. (2010), "Progressive finite element model calibration of a long-span suspension bridge based on ambient vibration and static measurements", *Eng. Struct.*, **32**, 2546-2556.
- Wilson J.C. and Gravelle W. (1991), "Modeling of a cable-stayed bridge for dynamic analysis", *Earthq. Eng. Struct. D.*, **20**(8), 707-721.
- Yang, Y.X. and Ge, Y.J. (2012), "Vortex-induced vibration and aerodynamic countermeasures for long-span cable-supported bridges with twin box girder", *Proceedings of the 18th IABSE Congress*, Seoul, September.
- Zhang, Z.T., Ge, Y.J. and Chen, Z.Q. (2014), "Vortex-induced oscillations of bridges: theoretical linkages between sectional model tests and full bridge responses", *Wind Struct.*, **19**(3), 233-247.
- Zhu, L.D., Xiang, H.F. and Xu, Y.L. (2000), "Triple-girder model for modal analysis of cable-stayed bridges with warping effect", *Eng. Struct.*, **22**(10), 1313-1323.